

ICRF plasma production with the W7-X like antenna in the Uragan-2M stellarator

Yu.V. Kovtun^a, V.E. Moiseenko^{a,b}, A.V. Lozin^a, R.O. Pavlichenko^a, A.N. Shapoval^a, L.I. Grigor'eva^a,
D.I. Baron^a, M.M. Kozulya^a, S.M. Maznichenko^a, V.B. Korovin^a,
E.D. Kramskoy^a, N.V. Zamanov^a, Y.V. Siusko^a, A.Yu. Krasiuk^a, V.S. Romanov^a,
I.E. Garkusha^{a,b}, T. Wauters^c, A. Alonso^d, R. Brakel^e, A. Dinklage^e, D. Hartmann^e,
Ye. Kazakov^f, H. Laqua^e, S. Lazerson^e, J. Ongena^f, H. Thomsen^e, G. Fuchert^e
T. Stange^e, S. Kamio^g and the Uragan-2M Team

^a *Institute of Plasma Physics of the NSC KIPT, Kharkiv, Ukraine*

^b *V.N. Karazin Kharkiv National University, Kharkiv, Ukraine*

^c *ITER Organization, St. Paul-lez-Durance, France*

^d *Laboratorio Nacional de Fusion, CIEMAT, Madrid, Spain*

^e *Max-Planck-Institut für Plasmaphysik, Greifswald, Germany*

^f *Laboratory for Plasma Physics, ERM/KMS, Brussels, Belgium*

^g *National Institute for Fusion Science, Toki, Japan*

The results of the plasma start-up with ICRH of U-2M RF discharges in H₂+He mixture with newly implemented controlled gas H₂ concentration are presented. The W7-X like ICRH antenna operated in monopole phasing with applied RF power of ~ 100 kW. We investigated plasma start-up in the pressure range $p = 6 \times 10^{-4} - 9 \times 10^{-2}$ Pa. Plasma production with an average density of up to $N_e \sim 10^{13}$ cm⁻³ was observed at frequencies the fundamental harmonic of the hydrogen cyclotron frequency.

Keywords: plasma production, ion cyclotron heating, stellarator, Uragan-2M, RF power.

1. Introduction

Stellarator research in the EUROfusion consortium focuses on optimized stellarators of the HELIAS (Helical Axis Advanced Stellarator) line [1]. Wendelstein 7-X (W7-X) in Greifswald, Germany, is the first HELIAS machine aimed to demonstrate plasmas at collisionalities and beta values relevant to the reactor conditions [2, 3].

Two other EUROfusion stellarators, TJ-II in Spain [4] and Uragan-2M (U-2M) in Ukraine [5], are of medium-size. They support the experimental programme of W7-X which plans to install the ion-cyclotron heating equipment [6, 7]. Main applications of the Ion Cyclotron Resonance Heating (ICRH) at W7-X is the generation of fast ions [8]. In addition, it can be used for wall conditioning, target plasma creation, and heating in the forthcoming campaigns of W7-X (starting in late 2022) [9].

The standard heating method at W7-X is second harmonic Electron Cyclotron Resonance Heating (ECRH) with the extraordinary 140 GHz waves at a central magnetic field of 2.5 T (X2 ECRH) [2]. In addition, ECRH at a lower magnetic field is envisaged to increase the beta-values achievable with the same amount of available heating power. The usage of the 140 GHz beams as 3rd harmonic

extraordinary waves (X3 ECRH) at 1.7T promises the same effective plasma heating in W7-X but needs at least a warm target plasma to operate [10].

The target plasma with necessary parameters could be created with neutral beam injection (NBI) at W7-X. But calculations [11] report on a delay of about 5 s between NBI start and full ionization of the neutral gas. This time is excessively long and would result in unacceptably high thermal load on the armour which the neutral beam hits. The successful NBI plasma creation during less than 0.5 s requires initial plasma with a density of $10^{10} - 10^{11}$ cm⁻³ [12]. Attempted X3 ECRH start-up, NBI start-up, and X3+NBI had no success on W7-X.

The initial target plasma for NBI can be created by the radio-frequency (RF) ICRH system of W7-X [6-8]. So the experimental studies and the theory show a need to develop ICRH start-up scenarios for W7-X at 1.7 T.

A two-strap antenna mimicking the W7-X antenna was installed on U-2M to support ICRH experiments at W7-X [5, 12]. In U-2M, the first research on plasma creation was carried out in helium [5]. The plasma density higher than 10^{12} cm⁻³ was produced near the fundamental hydrogen cyclotron harmonic. The key requirement for this scenario is the presence of minority ions in plasma for

which an ion cyclotron resonance zone exists in the plasma column. The major mechanism of plasma production is ionization by electron impact. The electron plasma component is heated by the slow wave (SW) [5]. At low densities plasmas are heated by SW directly excited by the antenna. Since the power needed for this is low, good antenna coupling to the SW is not necessary. At higher densities, the fast wave excited by the antenna converts to the SW at the Alfvén resonance layer. The SW propagates towards the lower hybrid resonance layer, where it is fully absorbed.

The scenario developed at U-2M [5] was qualified for ICRH plasma generation in the Large Helical Device [13]. The LHD experiments demonstrated the possibility to use ICRH plasma creation scenario [5] at large toroidal stellarator type devices.

This paper presents new findings from U-2M on RF discharge production in He atmosphere with hydrogen minority, as a continuation of the work that was initiated in [5]. Dramatically improved results emerge from RF discharges in H₂+He mixture with newly implemented control on H₂ concentration.

2. Experimental setup and diagnostic methods

The experiments were carried out at U-2M (see fig. 1). U-2M device is a medium-size stellarator of torsatron type [5, 14, 15]. The major radius of the device is $R = 1.7$ m, the minor radius is $r_c = 0.34$ m, the average plasma radius is $r_p < 0.24$ m and the toroidal magnetic field at the toroidal axis is $B_0 < 0.6$ T.

The creation of a H₂+He gas mixture with different relative concentrations was carried out in the gas pre-mixing system of U-2M [16]. This system allows one to work at various gas flows rates in the U-2M chamber, while keeping a constant gas composition. The gas mixture is puffed into U-2M through the gas puffing system SNA-2-01 [16]. The percentage of He and H₂ in the mixture was derived through partial gas pressures measurements inside the vacuum chamber U-2M using a mass-spectrometer IPDO-2 (partial pressure meter omegatron OPPM-2) [16].

Plasma is created with the W7-X-like two-strap antenna that consists of two parallel poloidal straps (width is 0.06 m and the length is 0.6 m) [5, 12]. The antenna is used in monopole phasing and is powered by the Kaskad-1 (K-1) RF generator [17]. The RF generator anode voltage was varied stepwise as follows: $U_{a1} \approx 0.4 \times U_a$ at the start, $U_{a2} \approx 0.6 \times U_a$ at step 1 and maximal anode voltage U_a was set at step 2, shutdown is done at step 3. The RF power value was calculated according to the measurements of the forward and backward waves' amplitudes.

The average electron density is measured with the



Fig. 1. General view of stellarator Uragan-2M.

super-heterodyne interferometer at 140 GHz frequency [18]. The plasma optical emission was recorded with the monochromator-spectrograph SOLAR TII (SOL Instruments Ltd) model MS7501i (Czerny–Turner optical scheme) with a photomultiplier. The database in Ref. [19] was used to identify the optical emission lines. A poloidal scan of integral emission optical lines was made using 41 chords with uniformly distributed impact parameters, P , the vertical positions of the viewing line at the vessel major radius (see fig. 2). The optical line intensities are measured using a pulse-by-pulse technique. Separate optical diagnostic methods were used to determine the temperature of the electrons and ions. These measurements were taken along the central chord. The averaged electron temperature was determined from spectral line intensity ratios (line-ratio method) of He I (471.3nm) and He I (504.8nm) [20, 21]. The ion temperature was measured from the broadening of the spectral lines of ions He⁺ (He II 468.6nm) and C⁺ (C II 426.7nm) [20, 22].

3. Experimental results and discussion

The first experiments with the H₂+He mixture showed that the average density of the generated plasma is significantly higher than that obtained earlier in pure He [5]. For example, at the same injected RF power of ~ 90 kW ($U_a = 7.5$ kV, $f = 4.9$ MHz, $B_0 \approx 0.34$ T), the maximum average plasma density was $\approx 2.7 \times 10^{12}$ cm⁻³ in He and $\approx 8.3 \times 10^{12}$ cm⁻³ in the 25%H₂+75%He mixture, which is ~ 3 times greater in the second case. The initial pressure of the mixture (5.4×10^{-3} Pa) was ~ 20 times lower than the pressure (1.06×10^{-1} Pa) in the He discharge.

Fig. 3 shows typical time dependences of the RF power, average density, and spectral line intensities. In the time interval $t = 10$ -15 ms, the breakdown, creation of the preliminary plasma, and growth of the plasma density occur sequentially (see Fig. 3). The intensities of the He I, C II, and H _{α} spectral lines also increase. Further ($t = 15$ -18.5 ms) there is a further increase in the plasma density up to a maximum value of $\approx 1 \times 10^{13}$ cm⁻³, and the intensities of the He I, H _{α} spectral lines decrease, the C II line reaches its maximum value. With a decrease in RF power ($t = 18.5$ -

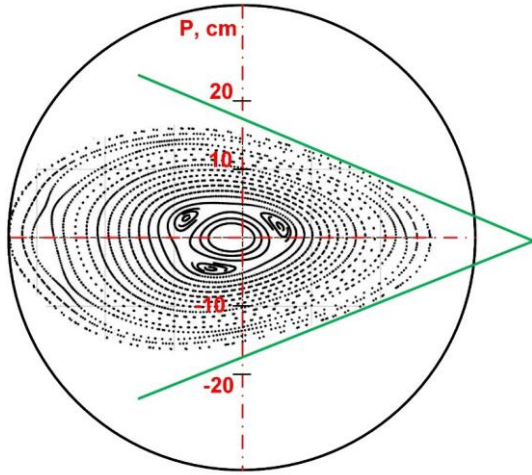


Fig. 2. Sketch of chord measurements in comparison to the vacuum flux surfaces at the particular toroidal position of U-2M. P is impact parameter.

25 ms), the plasma density decreases to a quasi-stationary value within $(7 - 8) \times 10^{12} \text{ cm}^{-3}$. After switching off the RF heating ($t = 25 \text{ ms}$) plasma decay begins, and the intensity of the spectral lines He I and C II increases after some time. This may be due to a decrease in the temperature of the electrons and, consequently, to the recombination of He^+ and C^{2+} ions.

The results of the chord measurements for the optical lines H_β , He I and He II are presented in figure 4 (for the location of the chords see fig. 2). In the experiments, the excited neutral atoms lines appear, first hydrogen (H_β) and, with a short time delay, helium (He I). Then the excited lines of the helium ion (He II) appear. As can be seen in fig. 4, the radiation sources have the same dimensions as the plasma column ($|P| < 15 \text{ cm}$). The maximum intensity of radiation is observed in the central region for all species.

The ionization energy threshold for He is 24.6 eV, for H is 13.6 eV and ions for He^+ is 54.4 eV, for C^+ is 24.4 eV, for C^{2+} is 47.9 eV [18]. Note that, as in [5], C IV and C V spectral lines were not observed. This is an indication of low electron temperature. The averaged electron temperature (determined by line-ratio method) was $T_e \sim 10\text{--}15 \text{ eV}$ for the plasma edge (13% H_2 +87%He, $B_0 = 0.346 \text{ T}$, $f = 4.9 \text{ MHz}$, $U_a = 7 \text{ kV}$, $p = 2.310^{-3} \text{ Pa}$).

The maximum temperature of the ions (measured from the broadening of the ion spectral lines) was $T_i \approx 23 \text{ eV}$ for C^+ (13% H_2 +87%He, $B_0 = 0.346 \text{ T}$, $f = 4.9 \text{ MHz}$, $U_a = 7 \text{ kV}$, $p = 2.35 \cdot 10^{-3} \text{ Pa}$) and $T_i \approx 18 \text{ eV}$ for He^+ (6% H_2 +94%He, $B_0 = 0.338 \text{ T}$, $f = 4.9 \text{ MHz}$, $U_a = 7 \text{ kV}$, $p = 2.35 \cdot 10^{-3} \text{ Pa}$).

Experiments in H_2 +He mixture showed that the maximum average plasma density depends on the percentage of H_2 in H_2 +He mixture and pressure at $U_a = \text{const} = 7 \text{ kV}$ (see

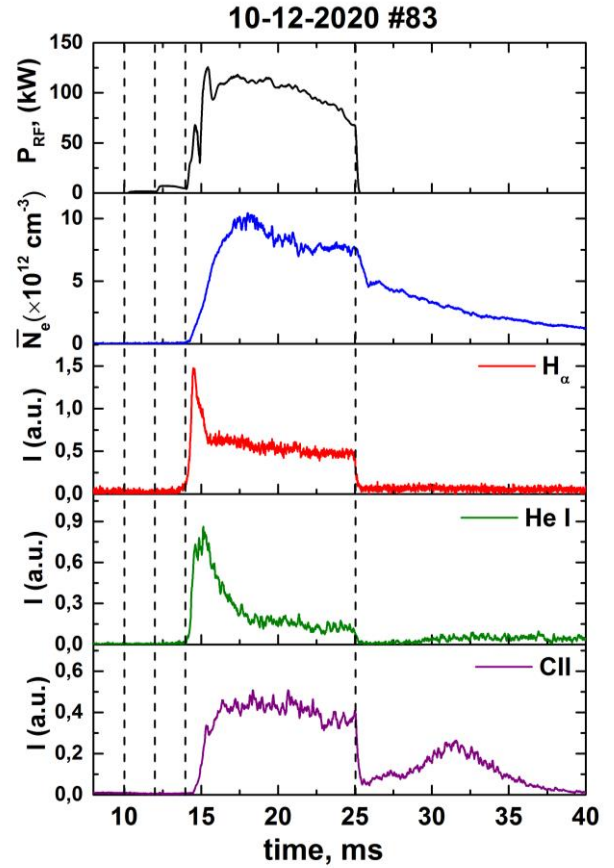


Fig. 3. Time evolutions of RF power; average plasma density; optical emission intensities of H_α (656.2 nm), He I, (447.15 nm) and C II (426.7 nm). ($U_a = 8 \text{ kV}$, $f = 4.9 \text{ MHz}$, $B_0 = 0.35 \text{ T}$, $K_\phi = 0.32$, working gas 14% H_2 +86%He, $p = 8.4 \times 10^{-3} \text{ Pa}$. The vertical lines show characteristic time moments of duty cycle of RF generator.)

Fig. 5). As can be seen in Fig. 5, the maximum plasma density of $9.8 \times 10^{12} \text{ cm}^{-3}$ is achieved at a pressure $p = 1.3 \times 10^{-2} \text{ Pa}$ in a mixture of 14% H_2 +86%He.

Decreasing the H_2 content in the mixture, as well as increasing its content in the mixture leads to a decrease in the maximum average plasma density. In all cases, regardless of the H_2 content in the mixture, there is a pressure range when the maximum plasma density is observed. For example, for a 14% H_2 +86% He mixture at a pressure range of 5.4×10^{-3} to $1.3 \times 10^{-2} \text{ Pa}$, a plasma density of $\geq 9 \times 10^{12} \text{ cm}^{-3}$ is observed. An increase in pressure above $1.3 \times 10^{-2} \text{ Pa}$ as well as a decrease in pressure below $5.4 \times 10^{-3} \text{ Pa}$ results in a decrease in plasma density. A similar situation is observed for other percentages of H_2 in the H_2 + He mixture (see Fig. 5). Better results in 14% H_2 +86% He mixture could be presumably explained by better RF power deposition profile.

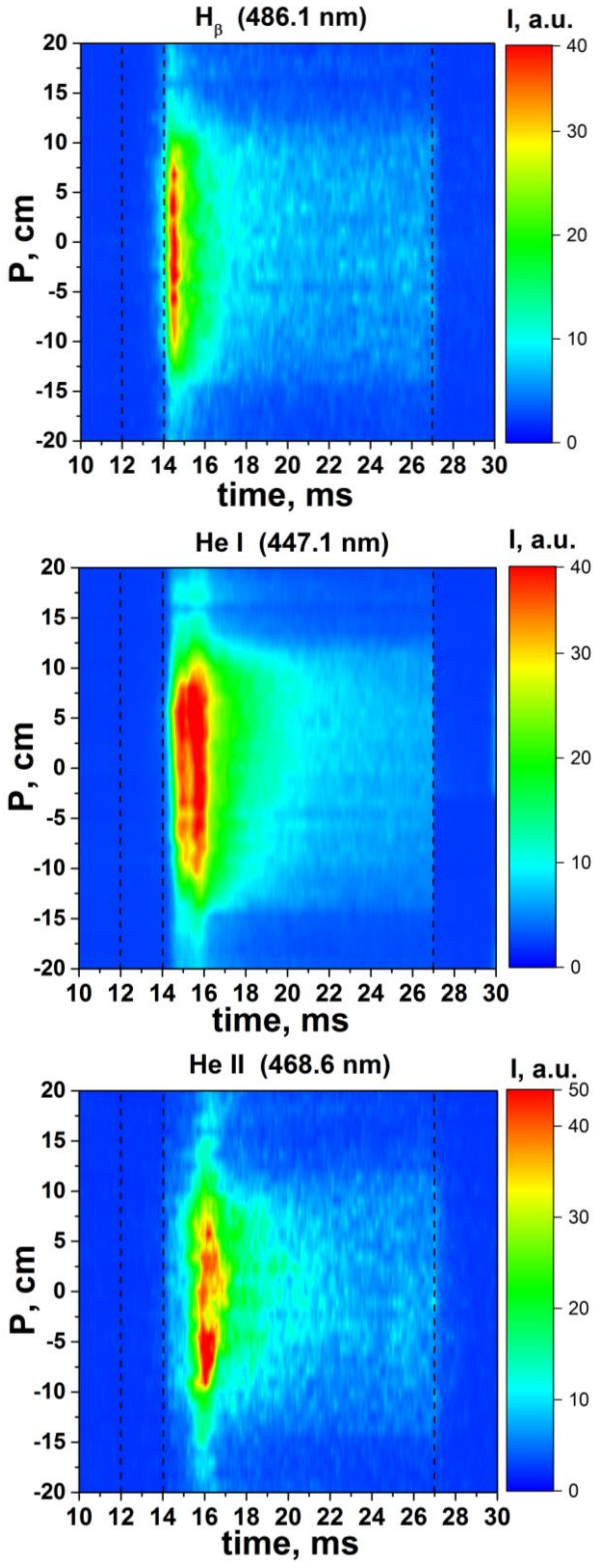


Fig. 4. Time evolution of H_{β} , He I and He II chord distribution. (12% H_2 +88%He, $B_0=0.335$ T, $K_{\phi}=0.324$, $f=4.9$ MHz, $U_a=7$ kV, $p=9.974\times 10^{-3}$ Pa. The vertical lines show time of duty cycle of RF generator.).

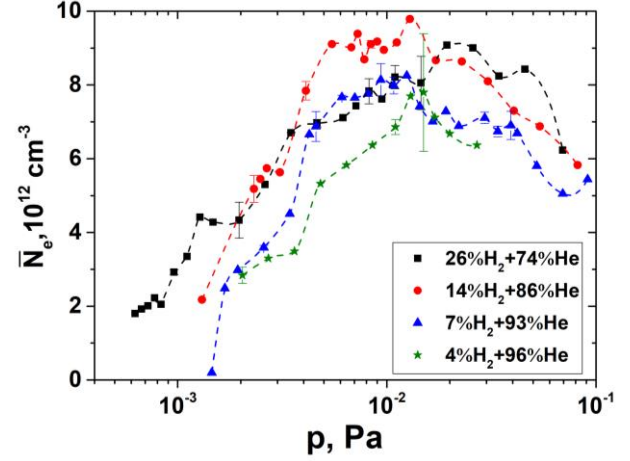


Fig. 5. Maximum average plasma density as a function of the pressure ($U_a=7$ kV, $f=4.9$ MHz). 26% H_2 +74%He ($B_0=0.34$ T, $K_{\phi}=0.326$), 14% H_2 +86%He ($B_0=0.35$ T, $K_{\phi}=0.32$), 7% H_2 +93%He ($B_0=0.35$ T, $K_{\phi}=0.32$), 4% H_2 +96%He ($B_0=0.344$ T, $K_{\phi}=0.32$).

4. Summary and conclusion

ICRF plasma production experiments with H_2 +He mixture can be summarized as follows:

- breakdown and plasma creation are achieved at lower pressure compared to pure He with similar RF power;
 - highest plasma densities can be obtained in plasmas with a gas fuelling mixture of 14% hydrogen in helium;
 - created plasmas have relatively high density ($\sim 10^{13}$ cm^{-3}) and low electron temperature (~ 20 eV);
 - optical emissions of H_{β} , He I and He II are more centralized in comparison with pure He experiments [5].
- The studied plasma production scenario is scalable and could be used in machines larger than U-2M. Such plasmas could be used as a target for further NBI heating. The results obtained here are important for preparing a scenario proposal for creating a target plasma at 1.7 T magnetic field in W-7X (further heating with NBI and X3 ECRH). Qualification of the scheme was conducted on LHD and will be continued in future experiments which will focus on optimizing the conditions for RF plasma creation.

Acknowledgment

This work has been carried out within the framework of the EUROfusion Consortium and has received funding from the Euratom research and training programme 2014–2018 and 2019–2020 under Grant Agreement No. 633053. The views and opinions expressed herein do not necessarily reflect those of the European Commission.

This work also received funding from National Academy of Sciences of Ukraine, Grant II-3-22.

- [1] *European Research Roadmap to the Realisation of Fusion Energy* (Programme Manager, EUROfusion, Garching/Munich, Germany, 2018).
- [2] T. Klinger *et al.*, Nucl. Fusion **59**, 112004 (2019).
- [3] G. Grieger *et al.*, Phys. Fluids B **4**, 2081 (1992).
- [4] E. Ascasibar *et al.*, Nucl. Fusion **59**, 112019 (2019).
- [5] V. E. Moiseenko *et al.*, J. Plasma Phys. **86**, 905860517 (2020).
- [6] J. Ongena *et al.*, Phys. Plasmas **21**, 061514 (2014).
- [7] J. Ongena *et al.*, AIP Conference Proceedings **2254**, 070003 (2020).
- [8] D. A. Castano Bardawil *et al.*, Fusion Eng. Des. **166**, 112205 (2021).
- [9] M. Endler *et al.*, Fusion Eng. Des. **167**, 112381 (2021).
- [10] N. B. Marushchenko *et al.*, EPJ Web Conf. **203**, 01006 (2019).
- [11] D. Gradic *et al.*, Nucl. Fusion **55**, 033002 (2015).
- [12] A. V. Lozin *et al.*, Probl. At. Sci. Technol. Ser.: Plasma Phys. **6**, 10 (2020).
- [13] S. Kamio *et al.*, Nucl. Fusion **61**, 114004 (2021).
- [14] V. Bykov *et al.*, Fusion Technology. **17**, 140 (1990).
- [15] O. S. Pavlichenko, Plasma Phys. Control. Fusion **35**, B223 (1993).
- [16] A. V. Lozin *et al.*, Probl. At. Sci. Technol. Ser.: Plasma Phys. **4**, 195 (2021).
- [17] V. B. Korovin and E. D. Kramskoy, Probl. At. Sci. Technol. Ser.: Plasma Phys. **6**, 19 (2012).
- [18] R.O. Pavlichenko *et al.*, Probl. At. Sci. Technol. Ser.: Plasma Phys. **1**, 257 (2017).
- [19] A. Kramida *et al.*, *NIST Atomic Spectra Database* (ver. ver. 5.7.1), (2019).
- [20] H. R. Griem, *Principles of Plasma Spectroscopy* (Cambridge University Press, 1997)
- [21] I. D. Latimer *et al.*, J. Quant. Spectrosc. Radiat. Transf. **10**, 629 (1970).
- [22] V. G. Konovalov *et al.*, Probl. At. Sci. Technol. Ser.: Plasma Phys. **4**, 53 (2002).